Numerical Weather Prediction

A Comparative Investigation into the Data Assimilation of Manual Bogus Data on Ex-Hurricane Gordon

Forecasting Research Technical Report No. 508

Adrian Semple

email: nwp_publications@metoffice.gov.uk

A Comparative Investigation into the Data Assimilation of Manual Bogus Data on Ex-Hurricane Gordon

Adrian Semple

Abstract.

During the extra-tropical transition of Hurricane Gordon when the depression was off the north-west coast of Spain, heavy manual bogussing was used in Operations Centre in attempt to produce a more accurate Global Model analysis. The resulting short-period forecast, during which the system crossed the Bay of Biscay, was observed to be poorer than one would have expected, with large implications for the forecast severity of the storm.

This report documents an investigation into the effect of the manual bogus data on both the analysis and the resulting short-period forecast. The study is carried out for two suite configurations to investigate if this impact differs as a result of continual model and system upgrades – PS11, operational at the time of the case, and PS15, operational at the time of writing.

The results show that in both PS11 and PS15 suites, the effect of the bogus data was to produce a short-period forecast with lower skill than if no bogus data was included in the assimilation. Further, the effect on the more modern suite configuration of PS15, was significantly more detrimental than the effect on PS11, with the result that the system was reduced to a shallow surface trough with little indication of a closed surface low. This shows a greater sensitivity of the more modern suites with respect to bogus data.

The investigation then goes on to study the assimilation of the bogus data in the PS15 suite in more detail. It is shown that the analysis and subsequent forecasts are highly sensitive to the assimilation of the bogus clusters with a large spread of central surface pressures resulting. This behaviour is not fully understood but has implications for the use of bogus data in this way.

History

Version 1.0	"A Comparative Investigation into the Data Assimilation of Manual Bogus Data on Ex-Hurricane Gordon"	15th October 2007
Version 1.1	Revised following comments by Andrew Lorenc and Tim Hewson	11th December 2007

1 Introduction

Operations Centre sometimes generate so-called ‘bogus’ data in an attempt to improve an analysis in which there is a perceived problem in the model. The bogus data will normally be based on satellite imagery, in which for example there is an apparent mismatch between model and the image, or else on observations which are not routinely assimilated. On other occasions it may be the creation of bogus observations which support existing data which it is felt critically reflect some developmental feature, whilst on other occasions the bogus data may reflect a bias which has been observed through examination of an observation-background timeseries. It is not clear how much impact this process has in modern NWP systems.

At 06z 21st September 2006, when the remnants of Hurricane Gordon were off the northwest coast of Spain, heavy manual bogussing was performed by Operations Centre in an attempt to produce an analysis in line with available observations. The short-period forecast obtained from this model run was observed to be of poor skill.

This technical report documents an investigation into the process of manual bogussing (which is a separate from the ‘automatic’ tropical cyclone bogussing) and its impact on the operational system at the time (PS11). The study aims to identify if the bogus data was correctly assimilated during the data assimilation process, and if so, to assess the impact of the data on the resulting analysis and forecast.

For comparative purposes, the experiments are also performed on the more recent operational configuration (PS15) to determine if the effects of bogus data observed in PS11 are stable as the sophistication of the operational system evolves through four upgrades.

2 Initial Testing of the Manual Bogus Process

Prior to any investigations discussed here, the process of creating bogus observations was tested on the medium range bench in the Operations Centre. A variety of bogus observations were generated which supported existing observations (which were generally in dynamically inactive regions for the purposes of this test). It was found that the bogus observations were able to be retrieved from the MetDB within minutes of their generation, and that their characteristics were as intended.

As bogus observations are treated as any other observation within the OPS (observation processing system) and VAR (the data assimilation system), this test suggests that the process of generating bogus observations on the Horace system (atleast via the Medium Range Bench) and their distribution to the MetDB is working correctly.

3 Meteorological Development

Hurricane Gordon formed in the North Atlantic Ocean on the 11th September 2006 and ran northwards around the western flank of the Azores High during the following days to be swept eastwards in the midlatitude flow from the 18th September. At this

time a broad upper trough occupied the North Atlantic with two embedded vortices; one in the western Atlantic and the other over northern UK.

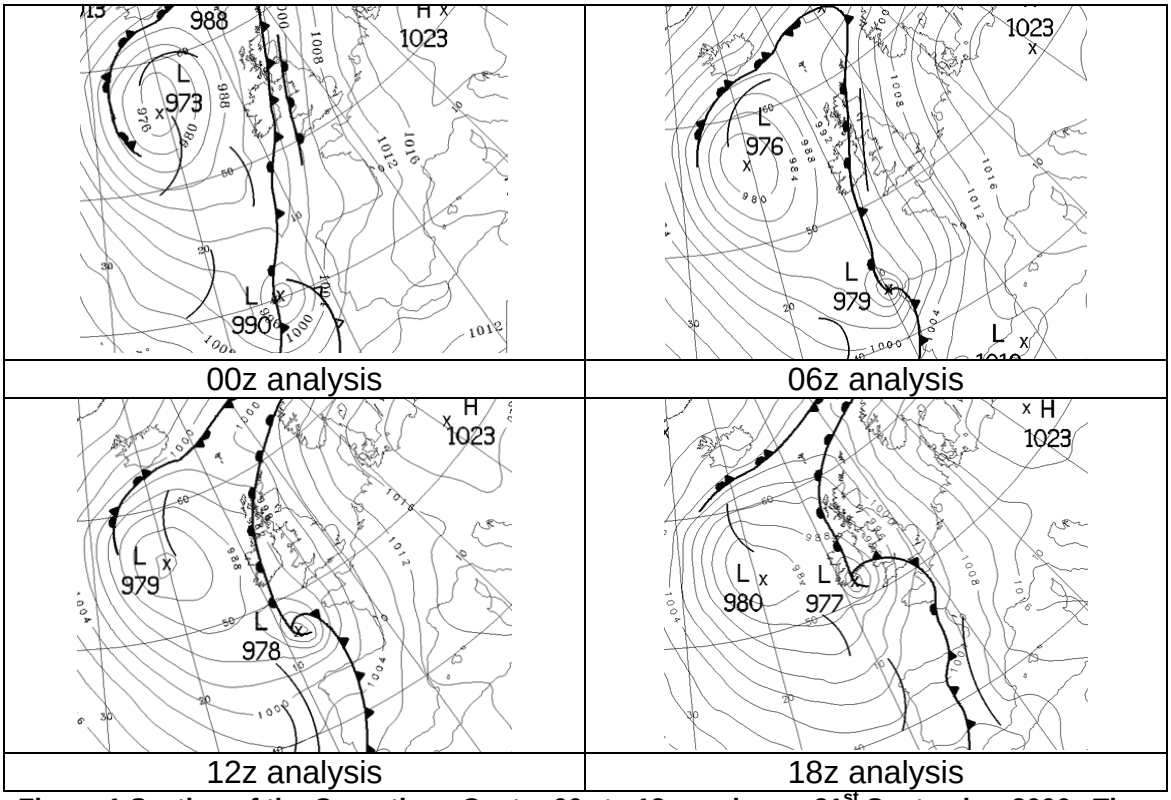

Figure 1 Section of the Operations Centre 00z to 18z analyses, 21st September 2006. The remnants of hurricane Gordon are moving north through the Bay of Biscay and towards Ireland during this period.

The vortex in the west emerged rapidly from the Davis Strait, with cyclogenesis well underway at the surface on the 19th and pushed south-east into the central North Atlantic with a deep large low (967) developing and becoming established to the west of the UK in the following days.

During the early hours of the 21st September, the remnants of Hurricane Gordon were engaged by the southern flank of the major upper vortex off the western coast of Spain, with the system undergoing an explosive deepening of ~11hPa in 6 hours in response (Figure1). The depression then moved rapidly north-eastwards within the strong flow on the forward flank of the major upper vortex, pushing through Biscay and into Ireland by the end of the day.

The system's development within the Global Model analyses during the 21st September is shown in Figure 2. The hurricane remnants within the warm theta-w plume (~20C) are visible to the west of Spain at 00z. The system is within the southerly flow on the forward flank of the major upper trough associated with the major depression to the west of the UK. The system is analysed to deepen by 5hPa in six hours to 06z. This results is an error of ~7hPa with respect to the Operations Centre analysis at this time. A further deepening of 4hPa is observed in the following six hours.

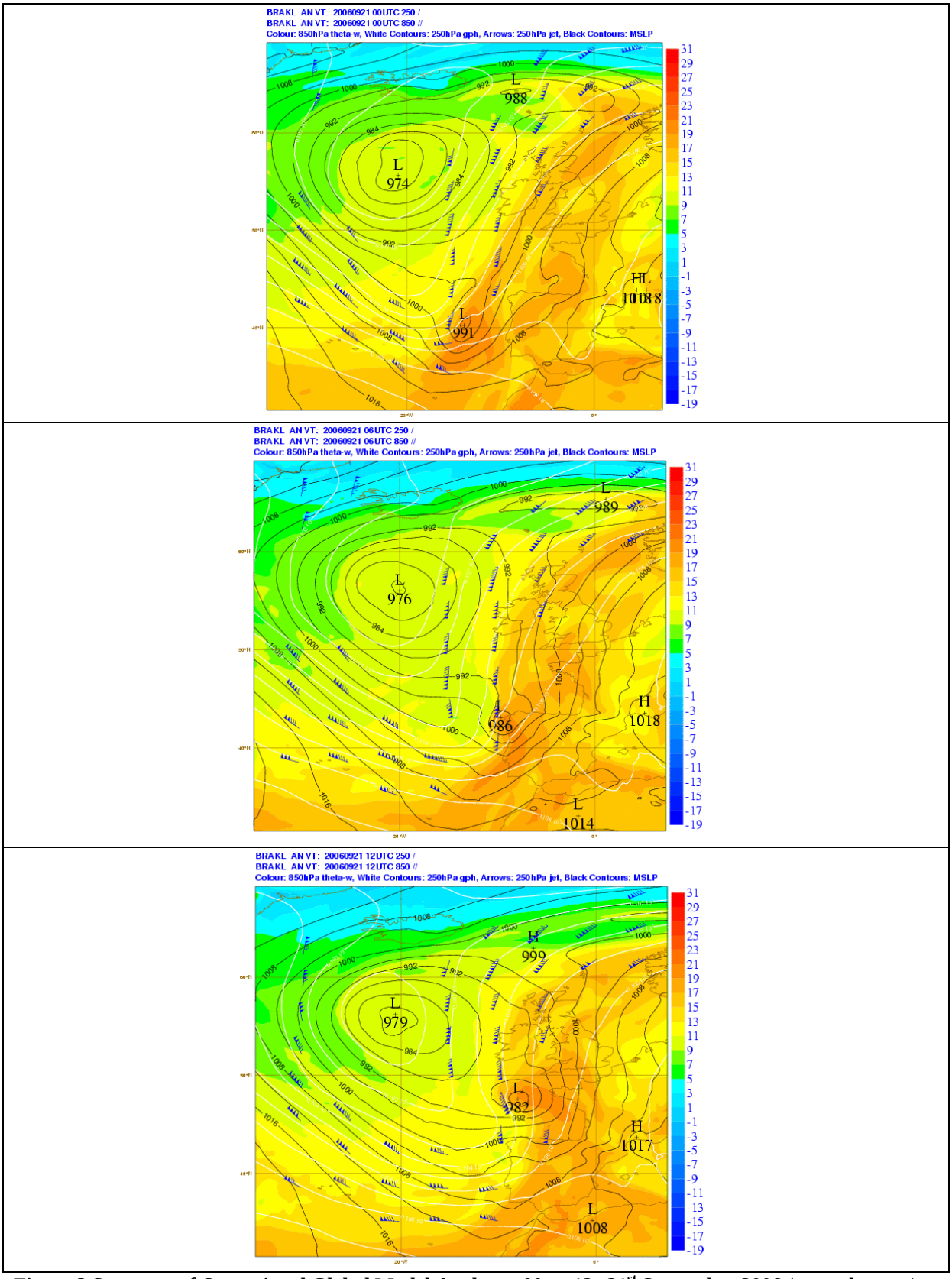

Figure 2 Sequence of Operational Global Model Analyses, 00z – 12z 21st September 2006 (top to bottom). The remnants of hurricane Gordon are engaged by the major upper trough early in the sequence with the system sweeping NE on the forward flank as a deepening feature. The analysis at 06z has an error of 7hPa with respect to the Operations Centre analysis.

4 Observations and Manual Bogus Data in the QG06 run

Figure 3 shows the surface-based observations available to the QG06 Global Model run. Of particular note are two observations to the west of Spain. These are made by the same ship V7HY7 which is moving south during this period and are in the direct track of the storm as it approaches from the southwest. The 04z observation is on the northern flank of the low, close to the centre and is the origin of the 60Kn southeasterly wind. By 06z the storm is near the northwestern coast of Spain (see figure 1), and so the ship observation at this time is on the southern flank of the low. This is the origin of the 30Kn northwesterly wind. Figure 4 shows the observation-background timeseries for the ship for the period of two days. Longer period O-B timeseries show that the ship is generally of good reliability. The graph shows that both the 04z and 06z pressure and wind observations have been accepted into the model for the operational run (rejections are curiously at later times of 09z and 12z, indicating problems at later times in the model background.).

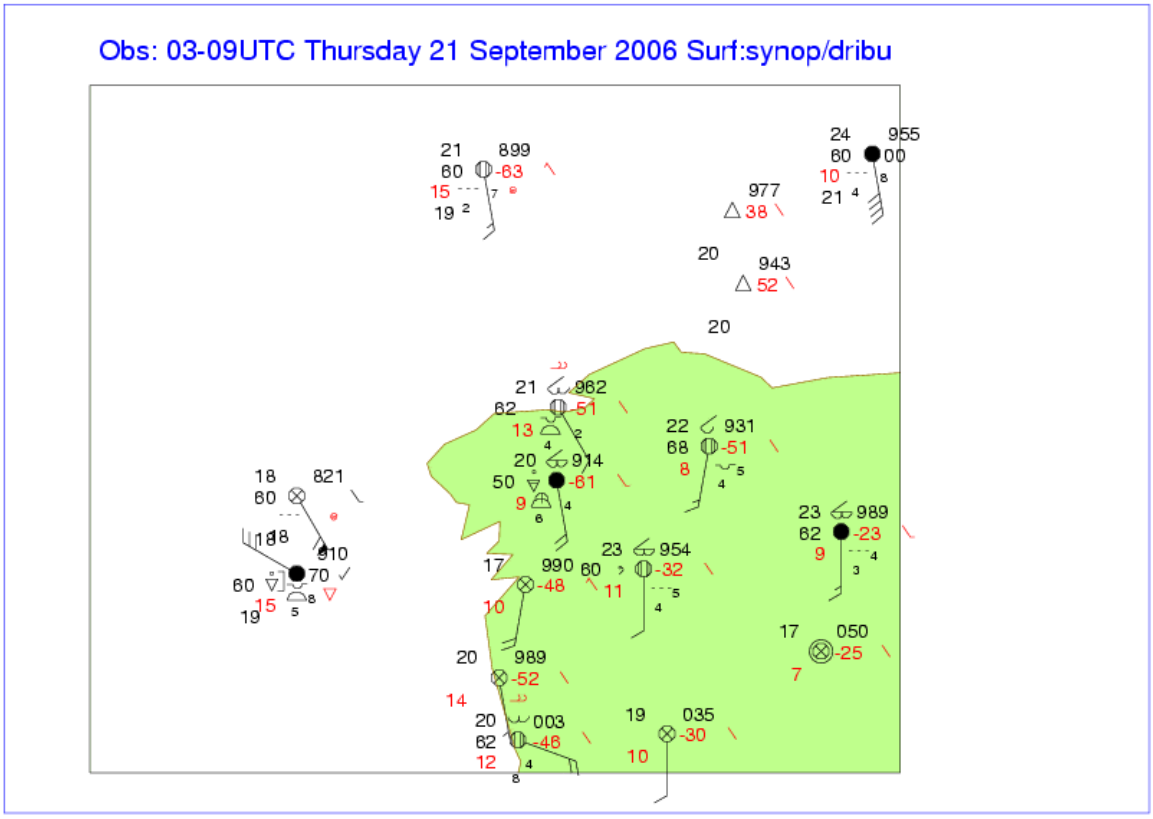

Figure 3 Surface-based observations available to the QG06 Global Model run on the 21st September 2006. Of note, the two observations to the west of Spain are made by the same ship V7HY7 at 4z (northern observation) and 6z (southern observation).

Retrieval of the Bogus data from the MetDB has shown groups of between three and six bogus surface wind and pressure observations have been created in an attempt to create a new surface low position off the northwest coast of Spain. These data are created with validity times of the supported observations. This new position of the low centre was based on available satellite imagery and Metar observations which would not have been assimilated by the model.

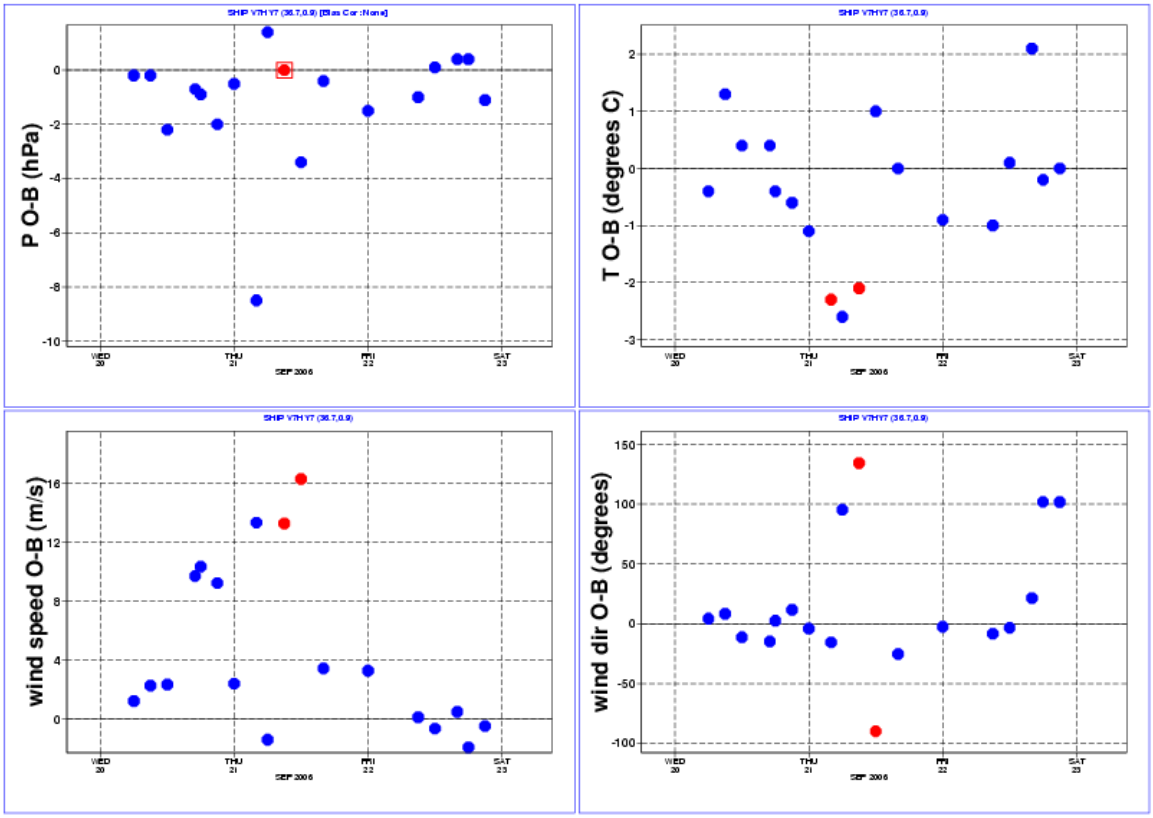

Figure 4 Observation-background timeseries for ship V7HY7 from the operational run. The 09z pressure observation is 16.7hPa below the background field and has been rejected in the quality control and suppressed to zero on the graph. The 09z and 12z wind observations have been rejected. BLUE: accepted, RED: rejected.

Figure 5 shows the contoured MSLP (a) T+6 background field and the (b) T+0 field valid at 06z 21st with coloured departure of the bogus observations from the respective field. The departure fields are calculated via an interpolation of the differences between the bogus point values and the model field onto the model grid. This normally gives a good indication of the main areas of departure of the observations from the model but can be 'smoother' than a distribution of the real point values.

Also plotted on the figure are the locations of the clusters of bogus observations. Comparing these with the observation plot in figure 3 shows that the northern, eastern and both southern clusters all support existing surface-based observations. This will be discussed further in the next section.

The positive/negative dipole in the departure field with respect to the background (Figure 5a) highlights the east-west location difference between the depression in the model field and that represented by the bogus observations. In general the observations are higher than the background in the west and lower than the background in the east. The point value departures of bogus observation MSLP and background field have been included on the figure in brackets.

The departure field with respect to the analysis (5b) shows that the contoured model analysis shows differences in the MSLP range upto ~9hPa to the west of the system, including differences of ~7hPa in the centre of the system. The analysis therefore indicates a significantly different system to that represented by the bogus data. This analysis is the combined effect of all observational data available to 4D-Var and so

the impact of the bogus data on the analysis cannot be determined without carrying out experimental reruns of the model including and excluding the bogus data.

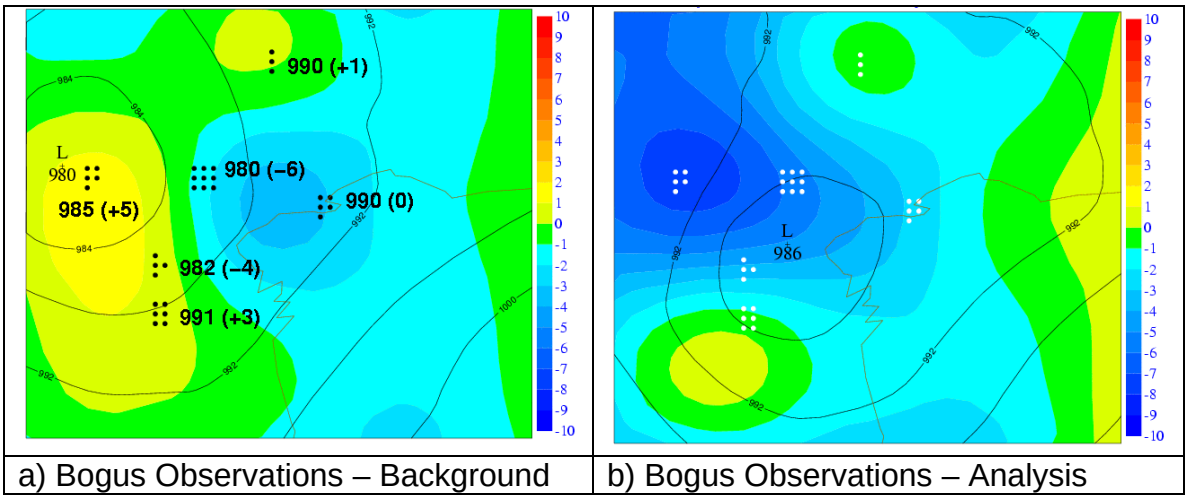

a) Bogus Observations – Background | b) Bogus Observations – Analysis

Figure 5 MSLP departures of bogus MSLP observations from (a) the background field and (b) the analysis for the operational run QG06 21st September. Positions of Bogus data are marked by black and white symbols. MSLP values are: 980 (middle group), 990 (eastern group), 985 (western group), 982 and 991 (southern groups), 990 (northern group). Winds are: calm (middle group), 9Kn 130deg (eastern group), 35Kn 310deg (western group), 29Kn 300deg (southern group), 15Kn 170deg (northern group). The point values of departures between bogus observation and model background field are shown in brackets in (a).

5 Global Model Rerun Experiments

Reruns of the Global Model have been performed in order to assess the impact of the bogus data on (a) the forecast and analysis system at the time, and (b) a more recent configuration of the model suite.

The configuration of suite components that were integral to the running of the operational suite during Hurricane Gordon (e.g. the version of the Unified Model, OPS, VAR, satellite biases, station lists etc) was equivalent to the configuration of Parallel Suite 11 (PS11). PS11 suites have therefore been used to run one set of Global Model experiments; a control run (with all data including the bogus data) and a 'no bogus' run with the bogus data excluded from the system.

At the time of this investigation, Parallel Suite 15 (PS15) was operational. This suite configuration has been used to observe the impact of the bogus data on a suite configuration that is more appropriate to the current time; again with a control run and a 'no bogus' run.

In both cases, the model has been ran from the operational PS11 QU00 T+3 start dump as archived to MASS. Obstores files were also retrieved and used in the reruns so as to reproduce as close as possible the conditions of the operational forecast.

No period of spin-up was allowed for the PS15 suite as the goal of the experiment was to observe the response of the new model configuration relative to the PS11 suite. This required running the model from identical starting conditions for the comparison to be valid and enabled the impact of the bogus data on the new suite configuration to be directly compared with the PS11 results.

Figure 6 shows the impact of the OPS on the observations in the two PS11 runs near the Gordon remnants. Figure 6a shows the data coverage of the control run. This shows six clusters of bogus observations (blue) to the northwest of Spain. Four of these clusters are close to or coincide with other types of observation: the two southern clusters (4 and 5) support ship V7HY7 and the northern cluster (6) supports ship PFAQ, whilst the eastern cluster (3) supports a land observation 08001. The central (1) and western (2) clusters show no conventional observation type in their location. This may be seen more clearly in figure 6b which shows the data coverage plots within the 'no bogus' run of PS11.

Figure 6c and 6d show the quality control 'decisions' as a result of the OPS for both pressure and the u-wind component. This shows that for pressure, cluster 4 has been rejected and for wind, cluster 3 has been rejected (as no wind observations over land are assimilated). The observations that have been supported by bogus clusters 5 and 6 have also been rejected. This, surprisingly, despite the acceptance of the bogus clusters of identical values.

Figure 6e and 6f show the results of the quality control in the absence of any bogussing. Figure 6d shows that the surface pressure observation associated with cluster 4 has been rejected, whilst all others have been accepted. Figure 6f shows that the wind observations associated with both clusters 4 and 5 have been rejected. Note that no assimilation of surface wind is carried out within the Global Model.

Quality Control results for the PS15 runs have also been analysed. These show identical results as those for PS11 with the exception that the eastern-most bogus u-component wind observation in cluster 4 is accepted in the PS15 suite.

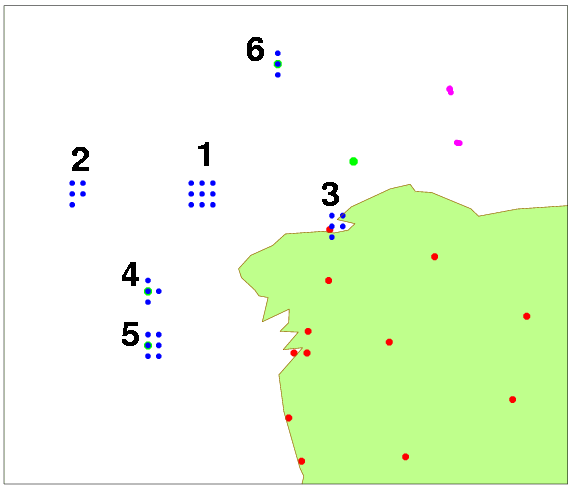

a) PS11 Cntrl Observation Types. BLUE: BOGUS, GREEN SHPSYN, RED: LNDSYN, PURPLE:BUOY. Numbers referred to in text.

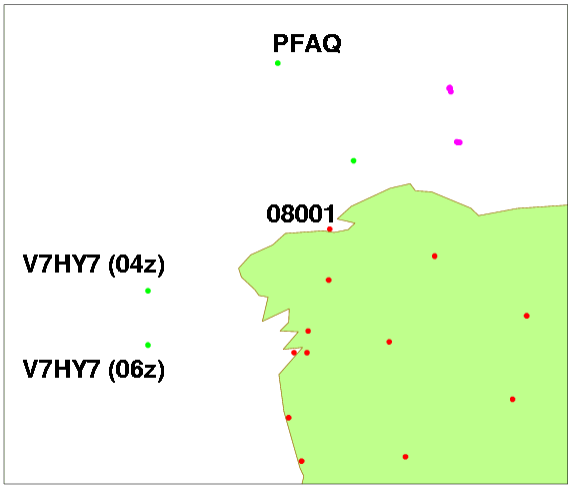

b) PS11 NO BOGUS Observation Types. BLUE: BOGUS, GREEN SHPSYN, RED: LNDSYN, PURPLE:BUOY. Station numbers for those associated with bogus observations are shown.

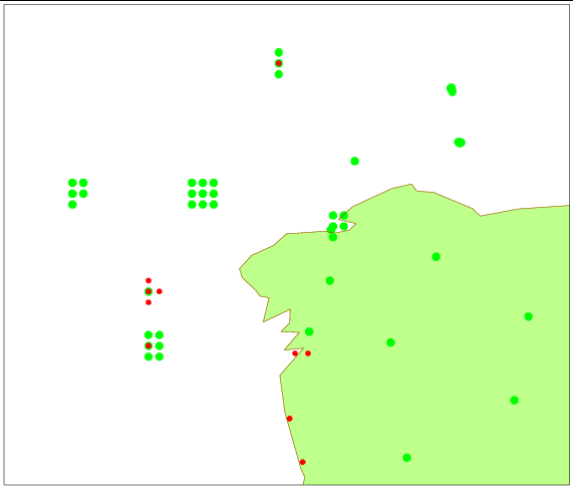

b) PS11 Cntrl Pressure Quality Control. GREEN: ACCEPTED, RED: REJECTED

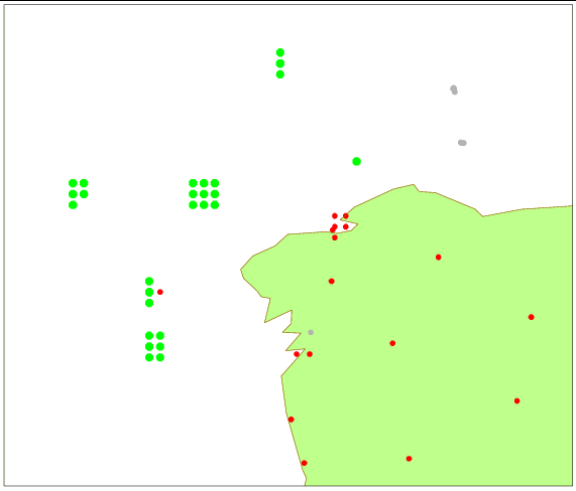

c) PS11 Cntrl U&V-wind Quality Control. GREEN: ACCEPTED, RED: REJECTED

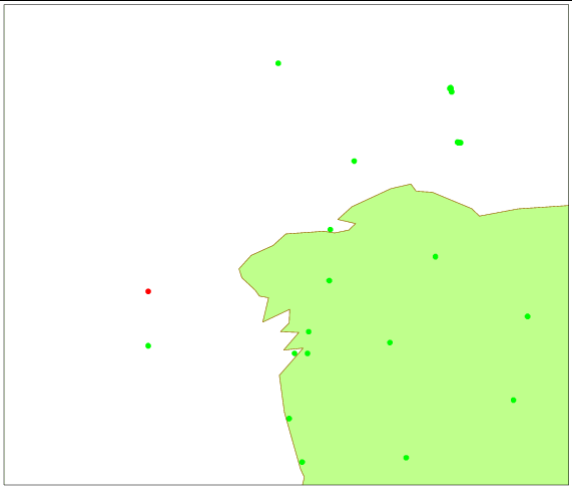

d) PS11 NO BOGUS Pressure Quality Control. GREEN: ACCEPTED, RED: REJECTED

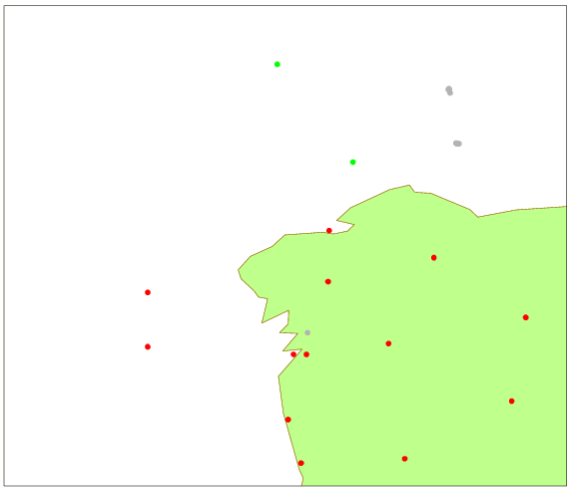

e) PS11 NO BOGUS U&V-wind Quality Control. GREEN: ACCEPTED, RED: REJECTED

Figure 6 Quality Control on the Bogus Observations in the PS11 rerun. (a) Shows the locations of all the data types available to the OPS. (b)-(e) Shows the results of the OPS quality control for pressure and U&V wind components for the Control and No Bogus Runs. PS15 results are identical with the exception that the rejected wind observation in bogus cluster 4 is accepted in PS15.

6 Impact of the bogus data on the analyses

4D-Var obtains a best fit of the available observational data with the model trajectory to produce an evolving analysis through the observation time window.
Analysis Increment fields (analysis-background differences) have been calculated to observe the impact of the observational data at the nominal analysis time (T+0). These have been calculated in terms of wind, geopotential height and temperature at three pressure levels (850hPa, 500hPa and 250hPa) and also in terms of MSLP. The impact of the bogus data on the analysis is then observed through a comparison of the analysis increments including and excluding the bogus data.

Figure 7 shows analysis increments for the control run (including the bogus data) for PS11 at 850hPa. Figure 8 shows increments for the PS11 suite in which the bogus data has been blacklisted.

The differences between the two figures show that the bogus data has been assimilated and that the effect is a southeastwards translation of the depression towards northwest Spain. This manifests itself as an increase in surface pressure and geopotential height to the rear of the system and a decrease ahead of it. This would be consistent with the positioning of the bogus data shown earlier. The increments in the control run also show the generation of a strong northwesterly low level jet increment (~50m/s) and a decrease in temperature of 11.5C which may be attributable to the advection of the colder airmass to the rear of the system as it translated bodily southeast.

The increments in the ‘no bogus’ run are generally similar to those of the control run but are significantly smaller: MSLP increases of ~5hPa, a northwesterly jet ~10m/s and temperature decreases of ~5C.

Figures 9 and 10 shows the increments for PS15 at 850hPa for both the control and the ‘no bogus’ run respectively. These increments are similar to those for PS11 although the main differences are evident on the southeastern flank of the system across western Spain. The PS15 control run shows smaller decreases in pressure increment here (2hPa c.f. 3.6hPa), which is associated with a larger surface pressure of ~987hPa (c.f. 985hPa in PS11 control run). There are also larger increases of temperature (4.6C in PS15 c.f. 2.4C in PS11), and a stronger northerly jet across northwestern Spain.

This extension eastwards between the two suites across Spain is not solely the result of the bogus data as it clearly shows up as differences in the two ‘no bogus’ runs for PS11 and PS15 (figures 8 and 10 respectively). This shows a different handling of the same data between the two suite configurations, with the more recent suite upgrades having more extensive effects.

Figures 11 and 12 show vertical cross sections through the geopotential height analysis increments for PS11 control and ‘no bogus’ runs, in which the section has been taken in a NW/SE line through the system. In these figures, the depression is at the centre of the figure. It is clear the analysis increments as a result of the surface bogus data are not localised to the surface but are extended vertically. This shows that the bogus data has had a significant and extensive impact on the analysis.

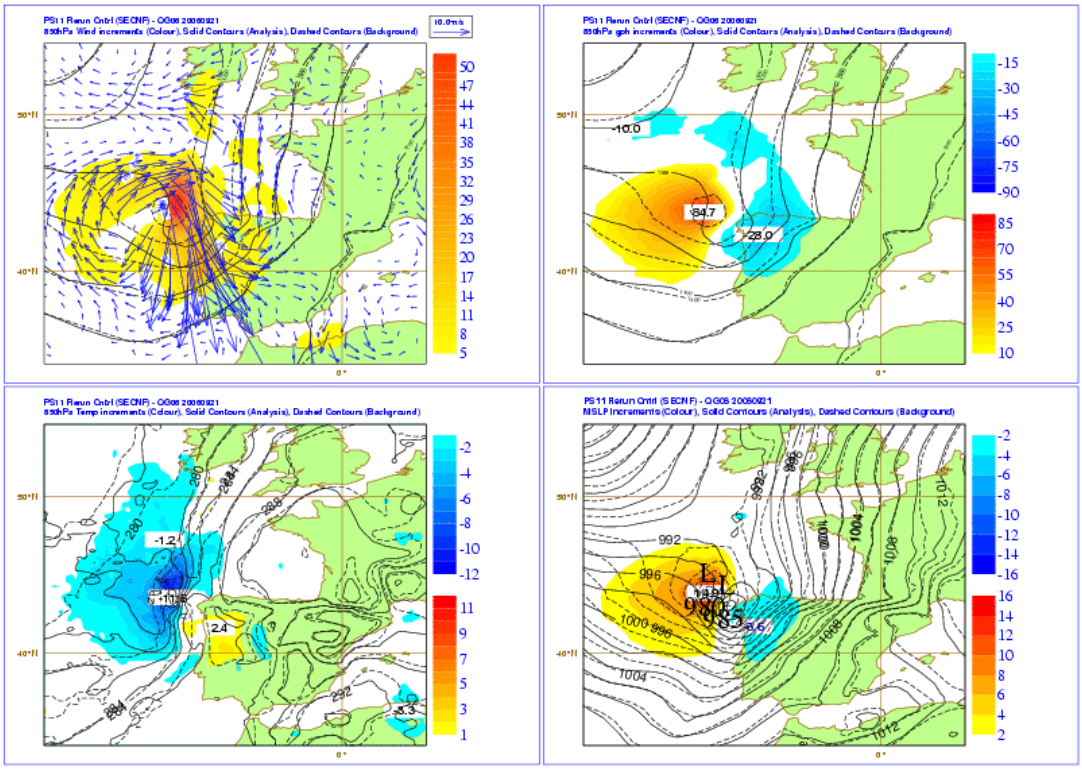

Figure 7 Analysis Increments (colour) for the PS11 Control run. 850hPa wind (top left), 850hPa gph (top right), 850hPa temperature (bottom left), MSLP (bottom right). Also shown: analysis field (solid) and background field (dashed) of the appropriate increment field. Wind increments are overlaid with the gph fields.

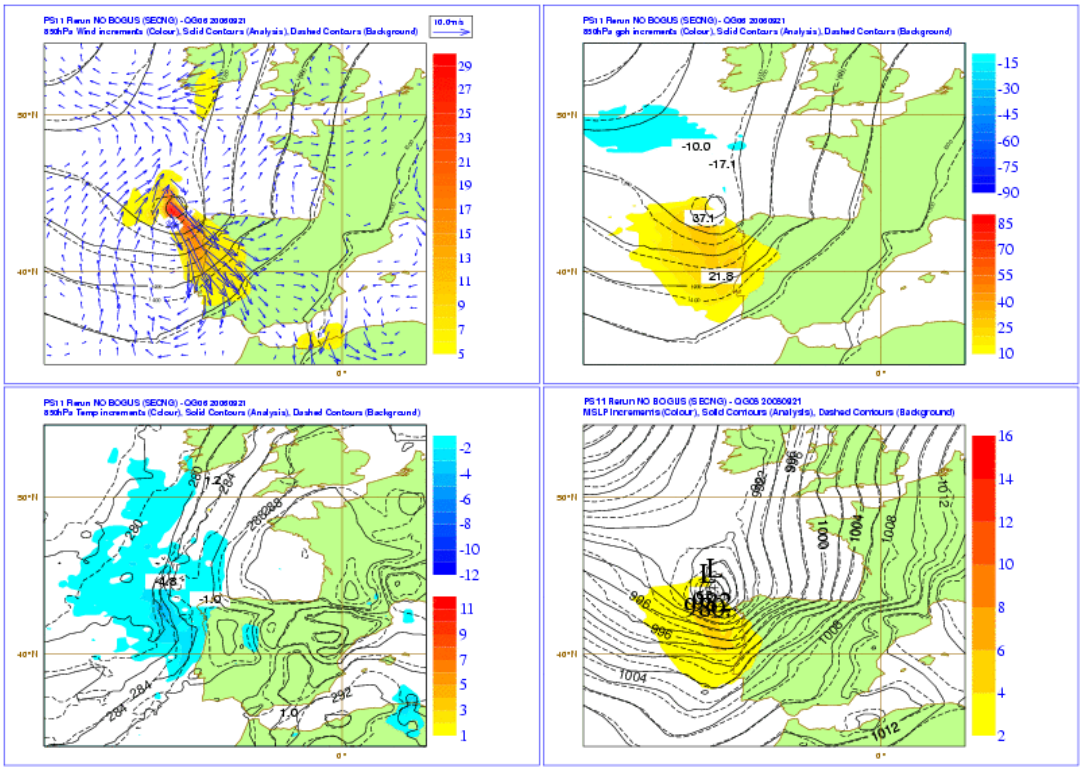

Figure 8 Analysis Increments (colour) for the PS11 'No Bogus' run. 850hPa wind (top left), 850hPa gph (top right), 850hPa temperature (bottom left), MSLP (bottom right). Also shown: analysis field (solid) and background field (dashed) of the appropriate increment field. Wind increments are overlaid with the gph fields.

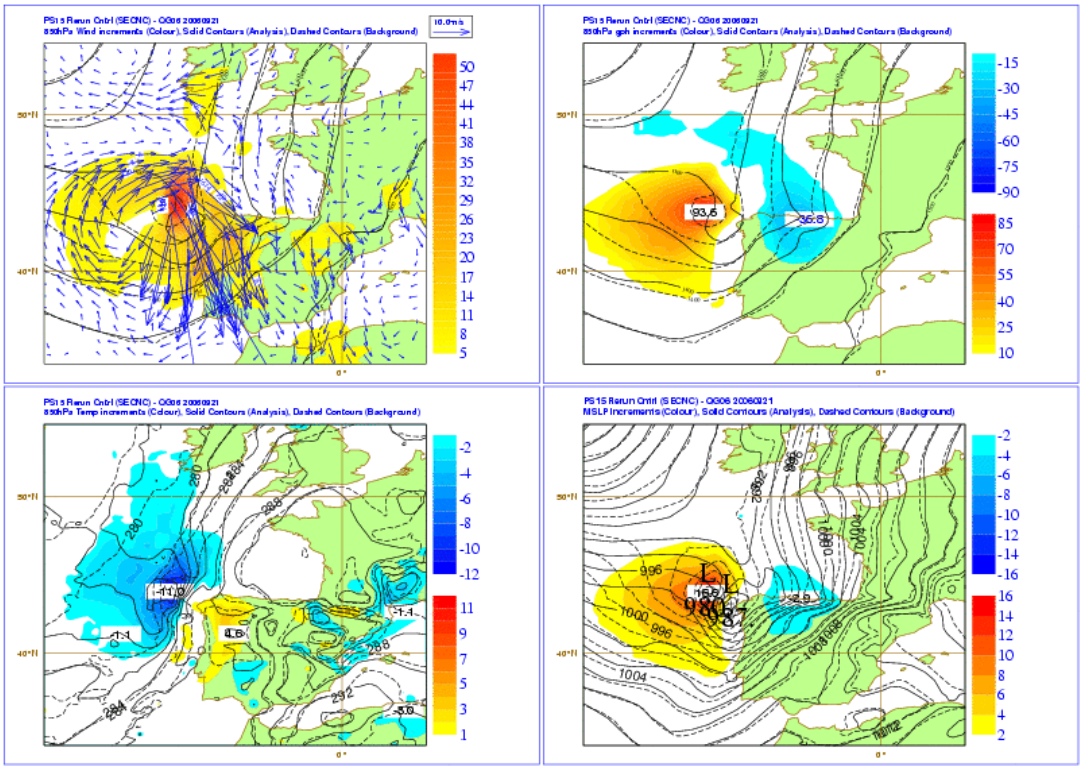

Figure 9 Analysis Increments (colour) for the PS15 Control run. 850hPa wind (top left), 850hPa gph (top right), 850hPa temperature (bottom left), MSLP (bottom right). Also shown: analysis field (solid) and background field (dashed) of the appropriate increment field. Wind increments are overlaid with the gph fields.

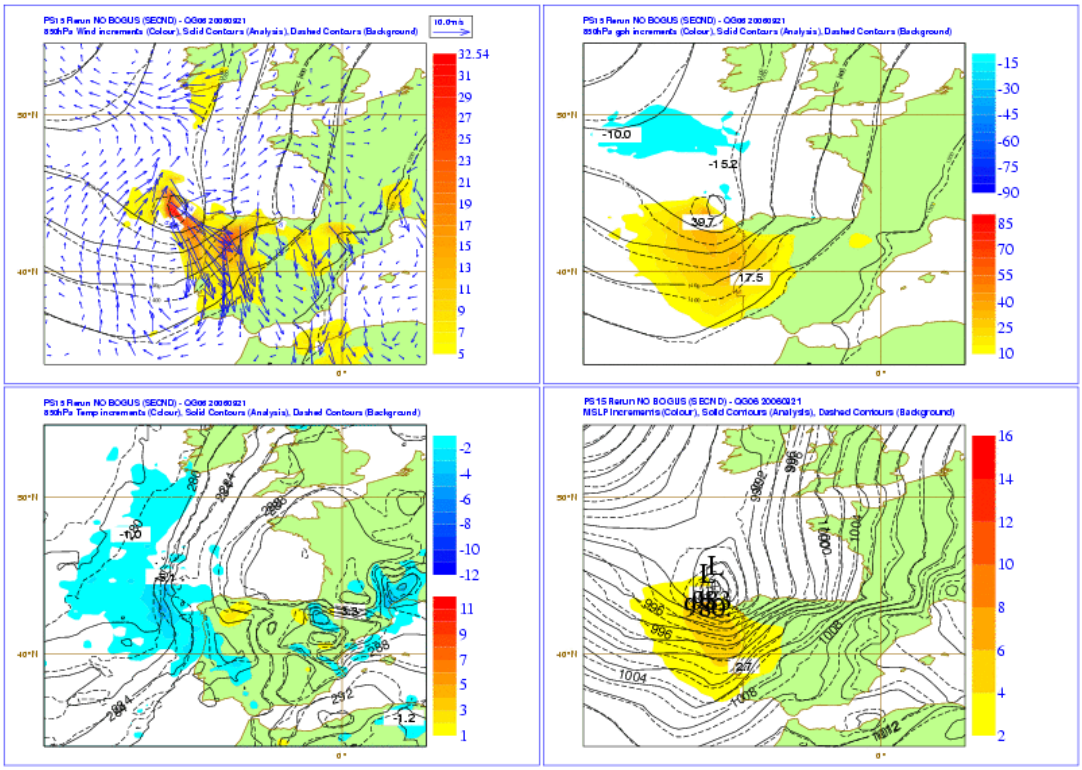

Figure 10 Analysis Increments (colour) for the PS15 'No Bogus' run. 850hPa wind (top left), 850hPa gph (top right), 850hPa temperature (bottom left), MSLP (bottom right). Also shown: analysis field (solid) and background field (dashed) of the appropriate increment field. Wind increments are overlaid with the gph fields.

Figure 13 shows the difference between the analysis increments between PS15 and PS11. Since the background field in each case is identical (each rerun was from the operational QU00 T+3 start dump), then these figures also represent the differences in the analyses between the two suite configurations. This shows that PS15 reacts by increasing the gph to the west of the system more relative to PS11, but by decreasing the gph to the E of the system (in the direction of translation of the low) less relative to PS11. The result is a deeper system in the PS11 case, as reflected in the MSLP of 2hPa deeper for PS11.

Figure 13 also shows that the PS15 analysis differences extend up to towards the top of the model, apparently breaking through into the stratosphere above 200hPa where increased stability results in more extensive horizontal modifications. Figure 14 shows the same PS15-PS11 difference but for the 'no bogus' runs. This shows that both the modifications to the stratosphere and the modifications to the east of the system at ~800hPa are due to characteristics of the PS15 suite relative to PS11, but that the large magnitude of the changes in these locations are a direct result of the bogus data and are not from some other data source.

Figures 15 and 16 show the v component on model levels in the analysis wind field for PS11 and PS15 respectively. There are significant differences east of 10W and below model level 16: the v component wind speed below ~model level 8 decreases rapidly in PS15 whereas it is maintained above 10m/s as low as model level 3 in PS11. This is a direct result of stronger low level northerly wind increments in PS15 over the Spanish landmass relative to PS11 (compare 850hPa wind increment fields in figures 7 and 9). The v component is also increased in PS15 by ~5m/s in the wind core at ~9W at model level 12. These differences suggest that there are significant changes between the model configurations over land, as the main differences all correspond to the area over the Spanish landmass (east of 9W). Changes over the North Atlantic (west of 9W) are relatively small.

The differences are highlighted further in figure 17 which shows the differences in the V component wind field between PS15 and PS11. The figure highlights the differences east of 9W. Further, it shows a sharp transition to the differences corresponding to ~model level 3. The differences in the model above Spain are also observed in the 'no bogus' runs. This shows that the bogus data are not entirely responsible for the differences, but are responsible for the amplification of the effect.

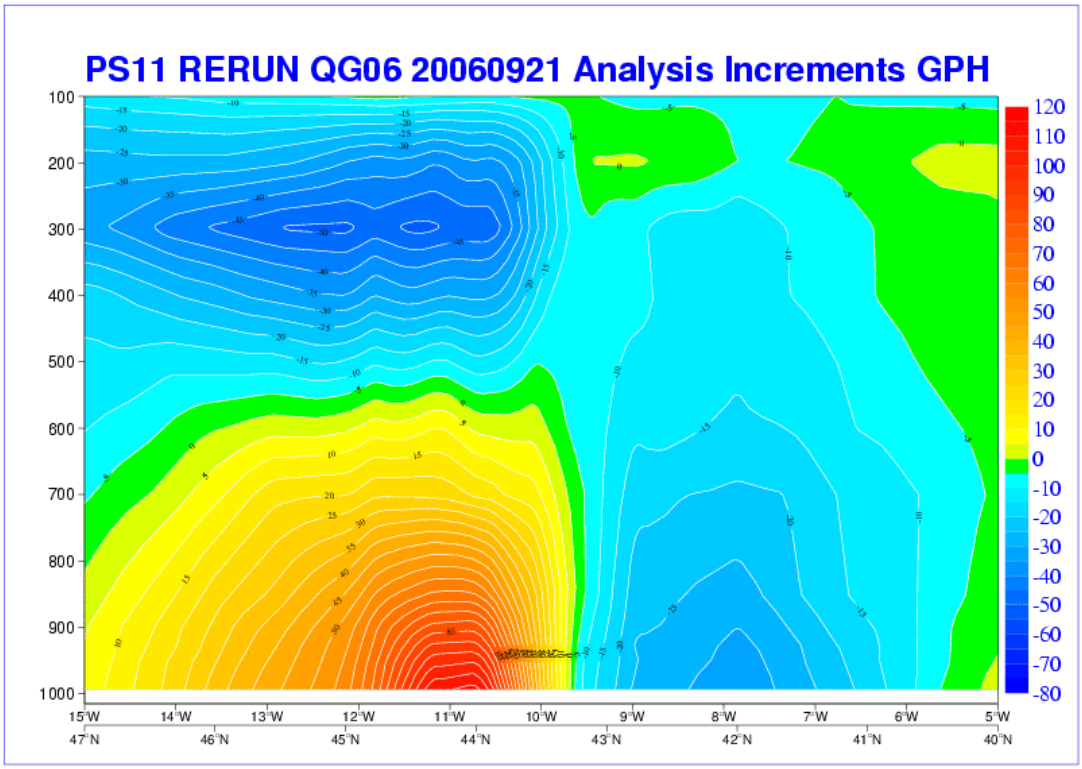

Figure 11 PS11 Control vertical cross section through the geopotential height analysis increment. The cross section runs NE/SW through the depression at 06z where the low centre is in the middle of the figure. This illustrates that the bodily shift from west to east of the system is consistent throughout the depth of the atmosphere.

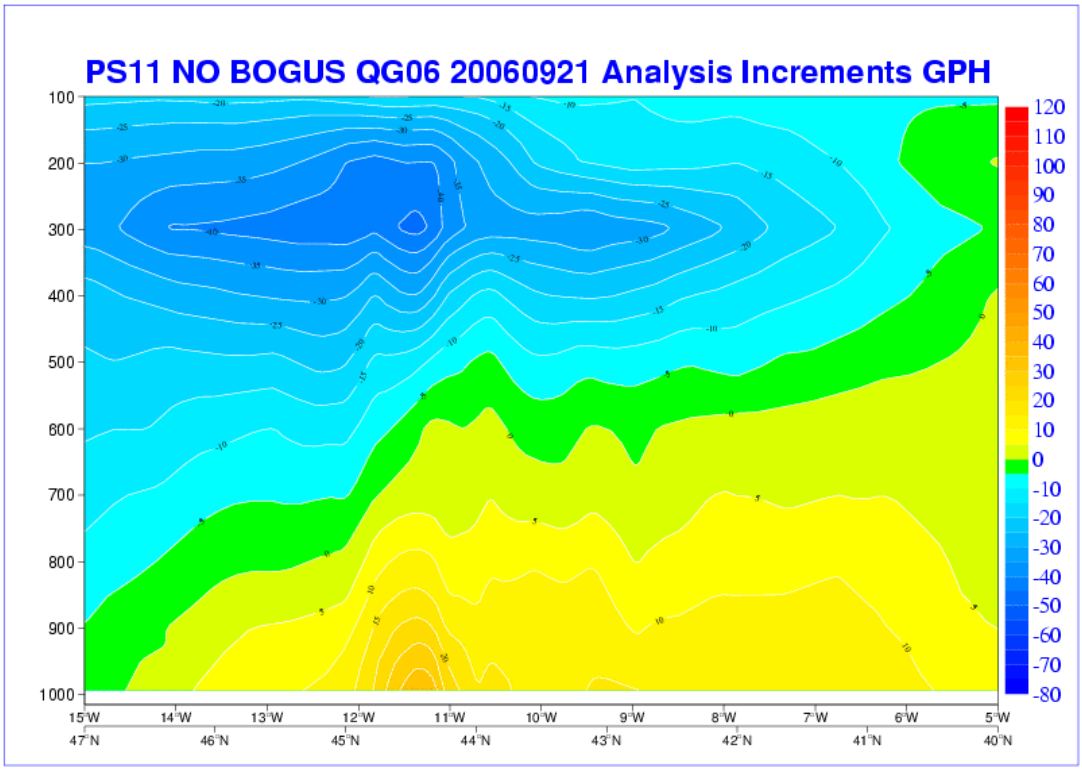

Figure 12 PS11 'No Bogus' vertical cross section through the geopotential height analysis increment, as figure 9. These increments show a small shift eastwards by the analysis, but do not show any deepening of the system. They strongly differ from figure 11.

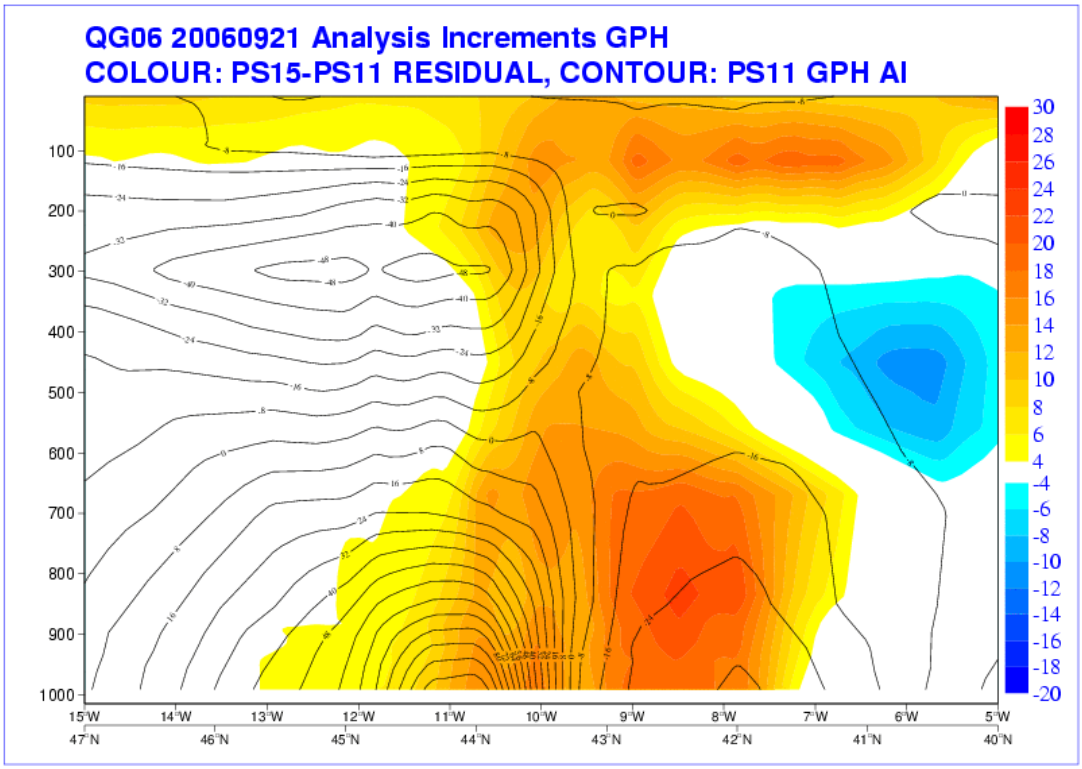

Figure 13 PS15-PS11 geopotential height analysis increment differences for both control runs containing the bogus data. PS15 does not decrease the gph as much as PS11 over land (east of 9W).

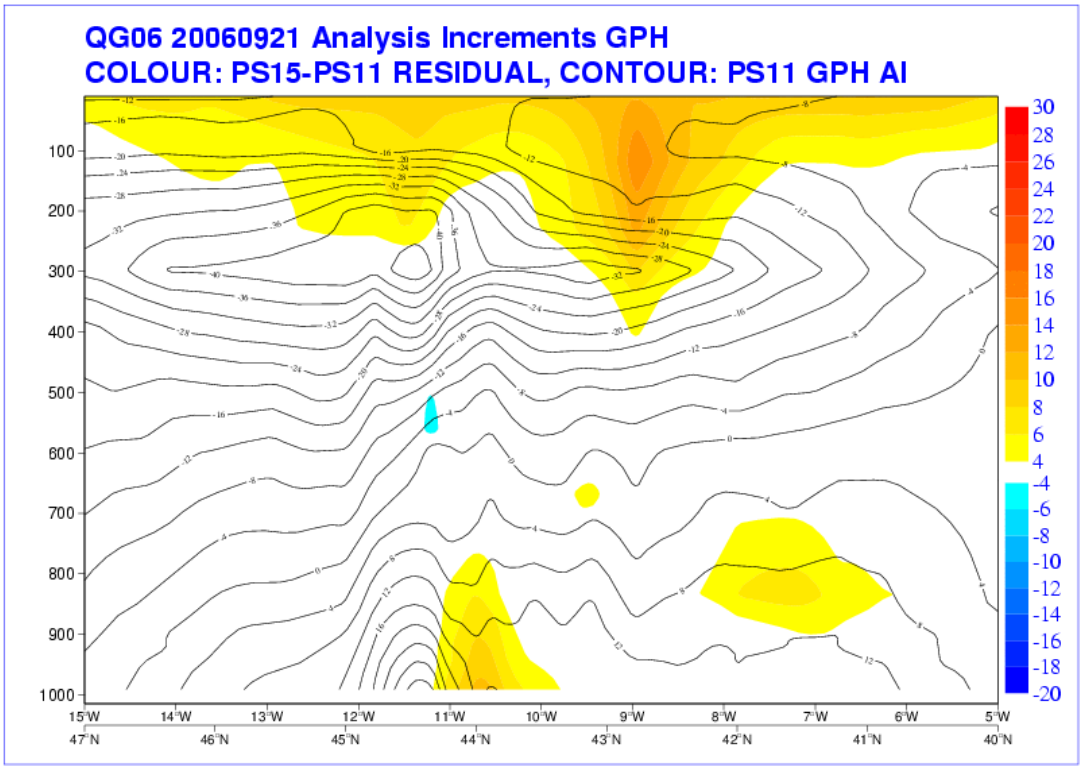

Figure 14 PS15-PS11 geopotential height analysis differences for both the 'No Bogus' runs. The gph over land remains larger in the PS15 case. The differences in the stratosphere remain but are significantly less than the PS11 case showing impact of the bogus data in the stratosphere.

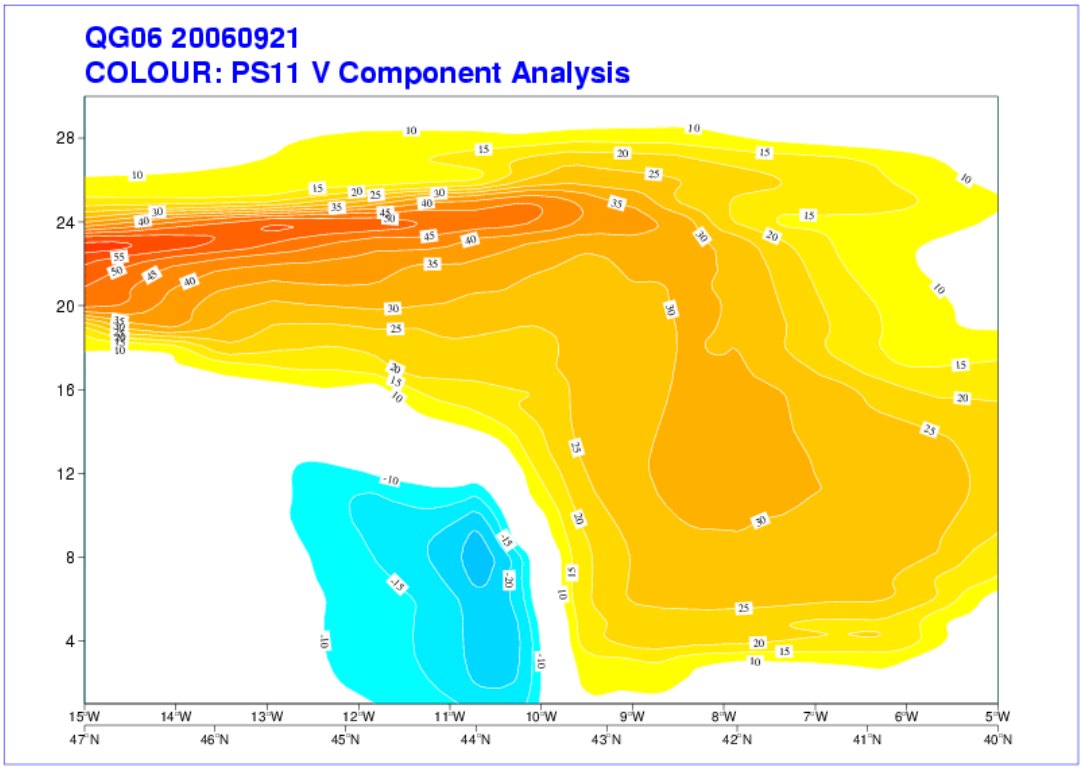

Figure 15 V component wind field in PS11 Control. The depression is in the centre of the figure, with the Spanish mainland extending eastwards from ~9W.

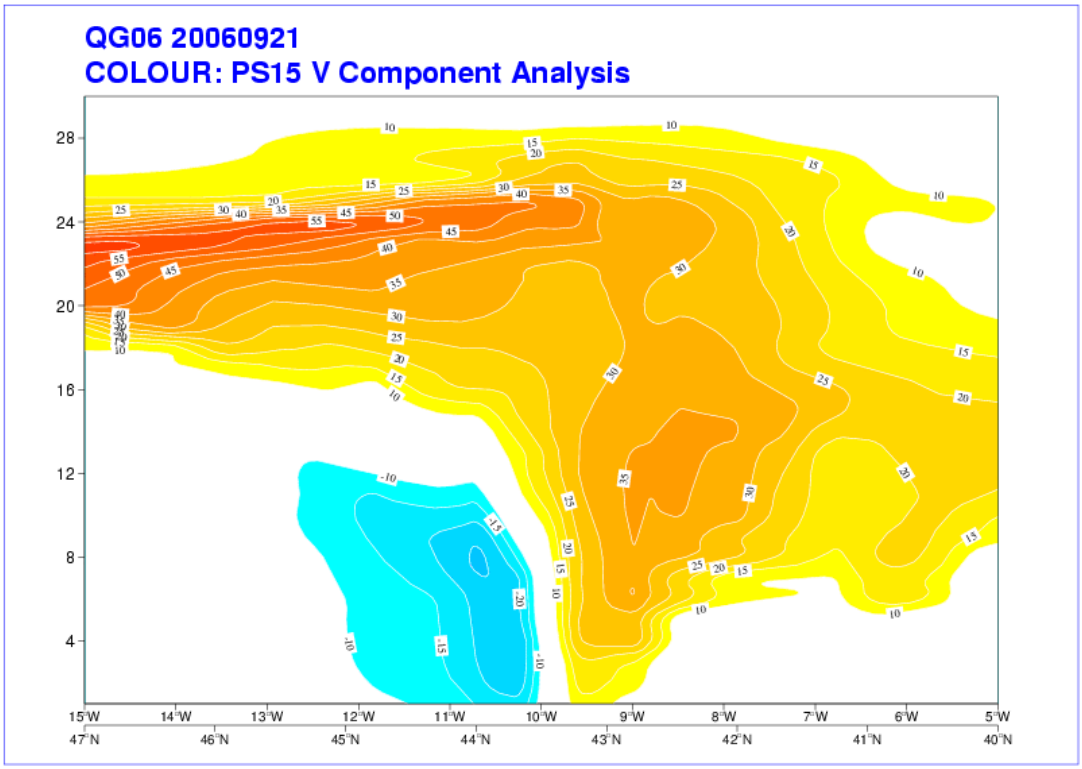

Figure 16 V component wind field in PS15 Control. The V component decreases rapidly over Spain below model level 8.

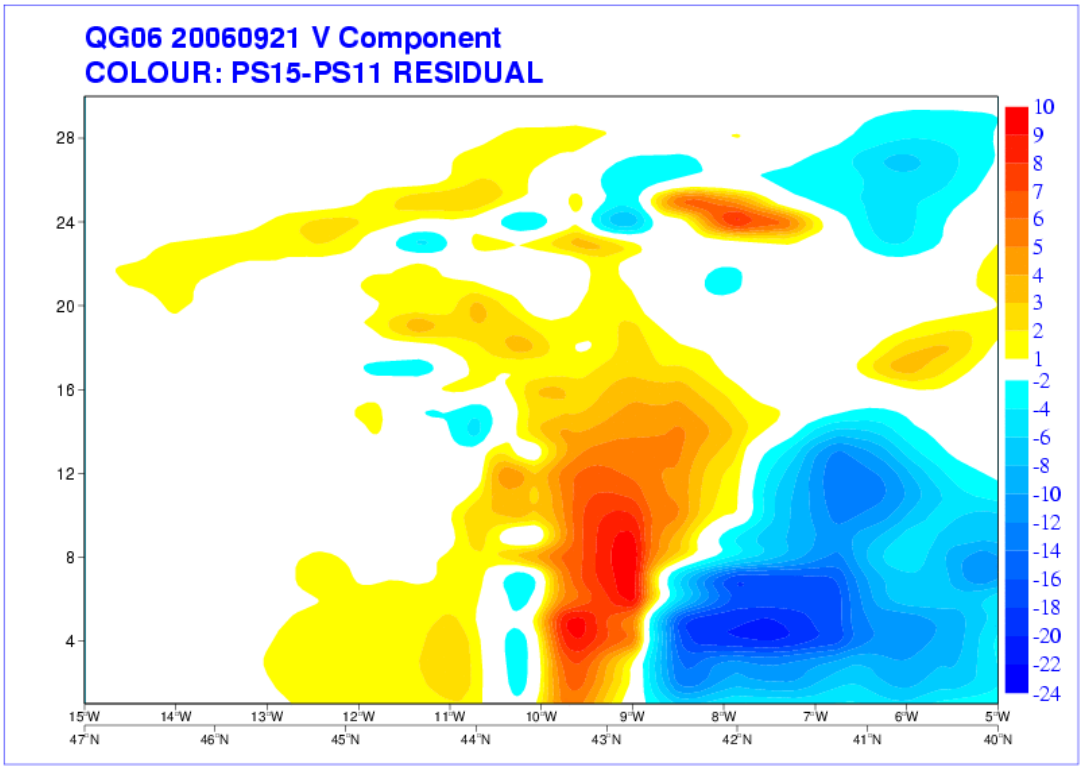

Figure 17 Differences between V component in the PS11 and PS15 suites. The large negative differences correspond to the area over Spain, with a sharp transition at ~model level 3.

There were several upgrades to the operational system between PS11 and PS15 which are likely to contribute to differences in model analysis and forecasts:

PS12 –

- **DA changes to improve resilience and optimisation (VAR22.3)**
- **OPS Upgrade (OPS22.3)**

PS13 –

- **DA Upgrade (VAR 22.4) including:**
  reduction in frequency of LS States to 1 per hour
- **OPS Upgrade (OPS22.4)**
- **Model upgrade including:**
  changes to convection for freezing level diagnosis and mid-level convection
  inclusion of non-orographic gravity wave parametrization
- **SA changes including:**
  Increase ATOVS observations

PS14 –

- **VAR upgrade (VAR23.1)**
- **OPS Upgrade (OPS23.1)**
- **SA changes including:**
  Introduce METOP data to replace NOAA15 data.

PS15 –

- **VAR upgrade (VAR23.2)**
- **OPS Upgrade (OPS23.2)**
- **UM upgrade including:**
  Adding a climatology of biogenic aerosols
  Corrections to convective clouds in the radiation scheme

It is not obvious from this which changes could account for the major differences between PS11 and PS15 observed here. Of the assimilation changes, this included additional use of AIRS and ATOVS observations. In this case, however, there were no AIRS observations assimilated in the critical region, and runs in which ATOVS data was excluded from the control runs showed only small impacts in the upper troposphere and none in the lower troposphere.

To identify if the differences could be attributable to the upgrades of the model physics, a set of runs were performed with no assimilation. The resulting T+0 fields were then a product of solely the differences between the model physics between the two suites, being a T+3 forecast from the T-3 start dump. It was found that the differences could almost entirely be attributed to the model physics changes in PS13 and/or PS15 and accounted for increased wind increments over land, with little or no differences over the sea. Further work is underway to understand these differences.

7 Impact of the bogus data on the forecasts

T+6 Forecasts

Figure 18 shows the T+6 forecast fields obtained from the experiments. The PS11 forecast including the bogus data (control) is observed as having an error of 6hPa relative to the Operations Centre analysis at 12z. When the bogus data is removed from the assimilation (18b), a deeper low is obtained with a more coherent centre and an error of 1hPa relative to the operations centre analysis.

The PS15 control run (18c) shows a system which has decayed in the six hours since the analysis time, with little indication of a closed surface low and with an error of ~11hPa. This may in part be due to the additional low-level weakening of the cyclonic circulation over Spain observed in the PS15 T+0 analysis discussed earlier. The PS15 rerun in which the manual bogus data was blacklisted shows a closed low with an error of ~3hPa relative to the operations centre analysis. There are little changes in positions between the four runs.

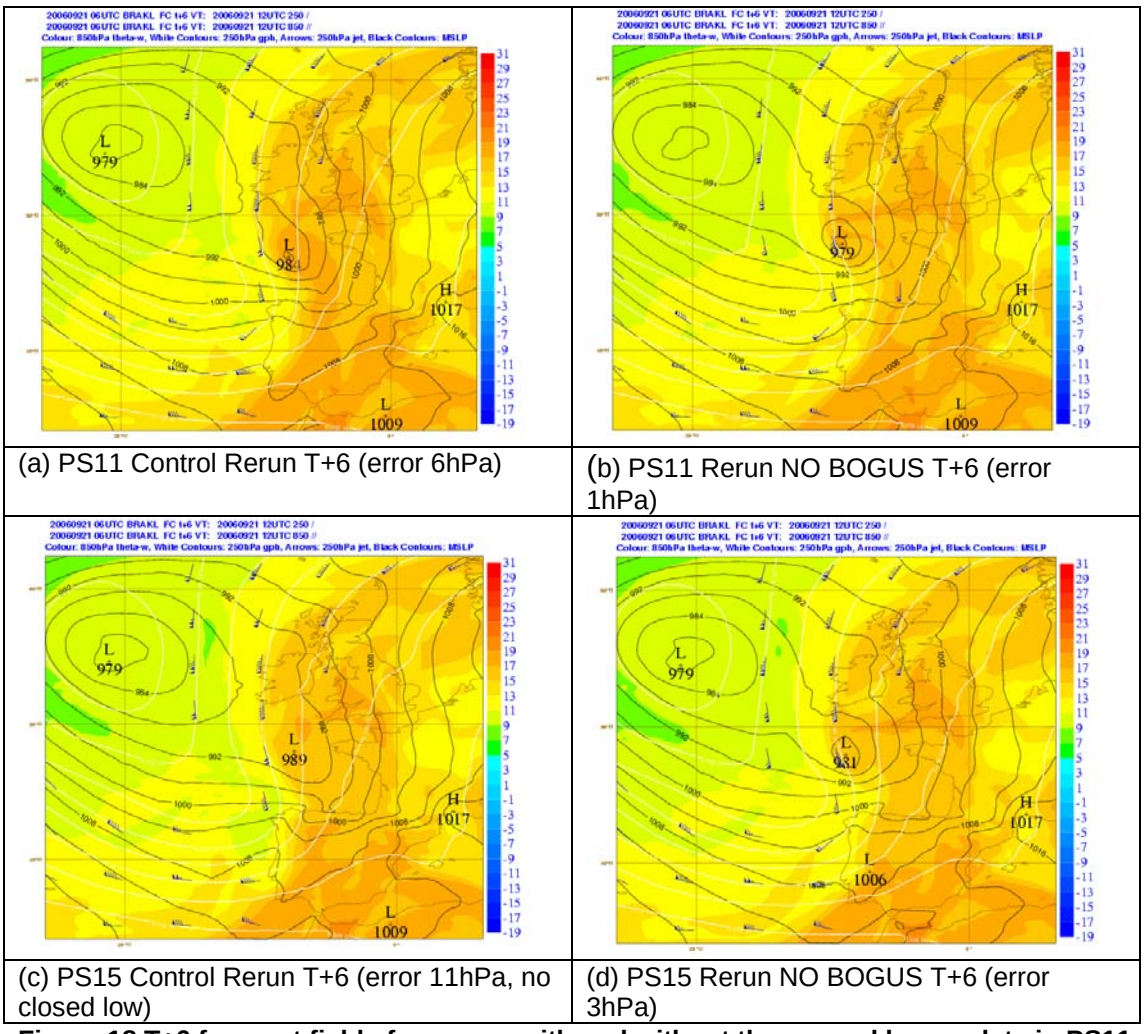

Figure 18 T+6 forecast fields for reruns with and without the manual bogus data in PS11 and PS15. In all cases the error with the bogus data (control) shows a larger error than that without the bogus data. In the case of PS15, the impact is larger than that of PS11, with little sign of a closed surface feature (c). The 'error' quoted is relative to the Operations Centre analysis.

These results are summarised in Figure 19 which shows the variation of central surface pressure for ex-hurricane Gordon within each of the four experimental reruns. In both suites, the run in which the bogus data is blacklisted, and therefore not included as part of the assimilation, shows behaviour which is closer to the operations centre analysis than the runs in which the bogus data is included. The large negative impact of the bogus data on the PS15 Control case is evident. A new assimilation cycle at 12Z is observed to draw the model runs into much better agreement.

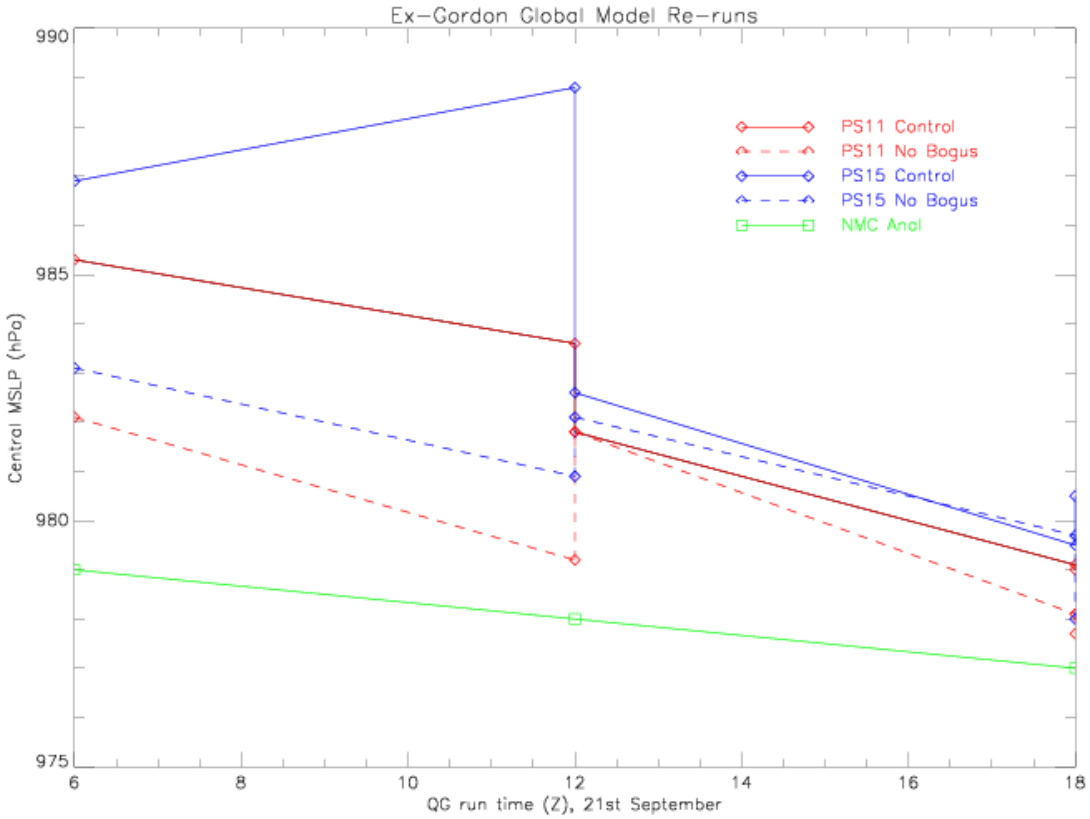

Figure 19. Variation of the central surface pressure of ex-hurricane Gordon as forecast within the different Global Model runs described in this study, 06z-18z 21st September. In all cases the 'NO BOGUS' run is closer to the NMC analysis. The effect of the bogus data on PS15 suite is to decay the system.

T+12 forecasts

Figure 20 shows the T+12 forecast fields, by which time the depression is near the southern coast of Ireland. The PS11 control run shows a low with a 2hPa error relative to the Operations Centre analysis (c.f. Figure 1), with the depression being too shallow. In contrast, the PS11 'no bogus' rerun shows a system which is 3hPa too deep. In terms of central pressure, this therefore shows less negative impact of the bogus data at T+12 than at T+6, with the model recovering somewhat. This is likely to be due to the larger scale model dynamics becoming dominant over the smaller structures introduced as a result of the bogus data.

The PS15 control run continues to show a surface trough with little sign of a closed surface circulation. The PS15 'no bogus' run shows the solution which verifies best of the four runs, with a depression that is only 1hPa too shallow. This is a good indication that the physics changes introduced into the UM at PS13/PS15 are

producing a superior forecast to the earlier PS11 UM forecast, but underlines the sensitivity of the PS15 model forecast to the bogus data.

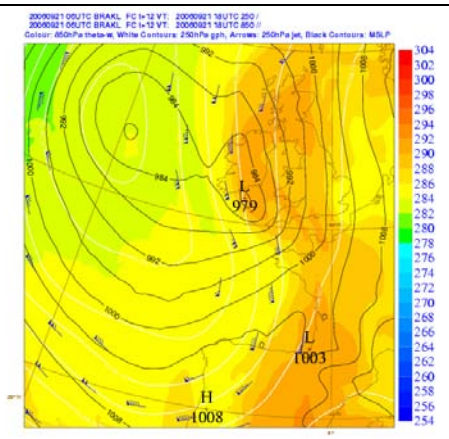

(a) PS11 Control Rerun T+12 (error 2hPa)

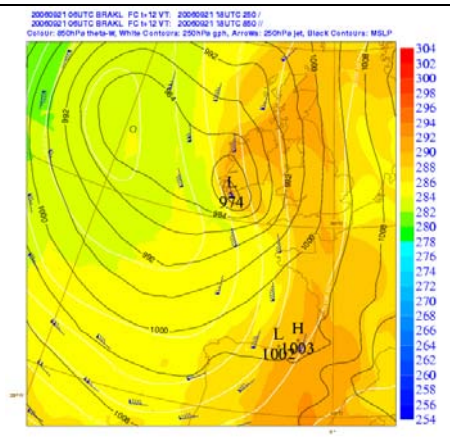

(b) PS11 Rerun NO BOGUS T+12 (error 3hPa)

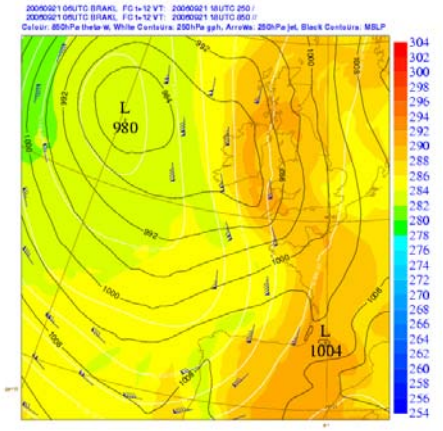

(c) PS15 Control Rerun T+12 (no closed low)

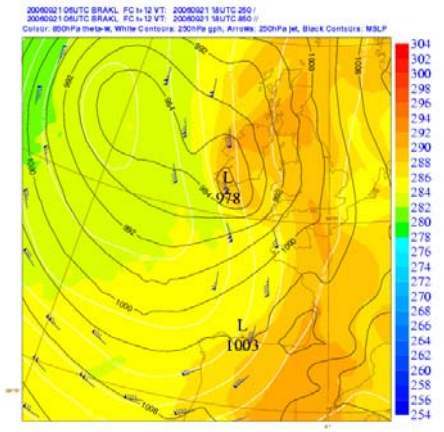

(d) PS15 Rerun NO BOGUS T+12 (error 1hPa)

Figure 20 As figure 15 but for T+12 forecast fields. The central surface pressure for the PS11 control run shows a system which is 2hPa too shallow relative to the Operations Centre analysis, whilst the 'No Bogus' run is 3hPa too deep. The PS15 Control run continues to show no closed surface low, whilst the PS15 'No Bogus' run verifies best of the four runs, with a 1hPa error.

8 Data Assimilation Experiments

It has been shown thus far that the assimilation of the bogus data resulted in a degraded analysis and short-period forecast of lower skill relative to a Global Model run in which no bogus data was assimilated. It was also shown that four of the six bogus clusters (3,4,5 and 6) supported existing observations and so were absolutely consistent with other real and local observations.

In order to investigate further the effect of the bogus data on the assimilation, a series of reruns were performed in order to observe the impact of each of the separate clusters on the analysis and forecast. This involved blacklisting five out of six of the clusters in each run. The experiments were performed on the PS15 suite only as this represented the most modern of the two suites under study.

Figure 21 shows the results of the quality control on each of the runs for pressure observations. Figure 21a and 21b reproduce the PS15 control and 'no bogus' runs for comparison. Figures 21c to 21h then show the results of the quality control when assimilating each of the different clusters of bogus observations 1 to 6 (numbers as shown in (a)). In most cases, the entire cluster is assimilated, with the exception of bogus clusters 1 and 4 in which two and one bogus observations within the clusters are rejected by the quality control respectively.

The assimilation of each cluster has different effects on the surrounding observations. For example, the assimilation of bogus cluster 1 (figure 21c) results in the acceptance of the ship V7HY7 at 04z but the rejection of the same ship at 06z (compare with figure 3). The assimilation of cluster 1 also results in the rejection of a SYNOP observation on the adjacent Spanish coastline with respect to the 'no bogus' run. The assimilation of bogus cluster 2 (figure 21d), however, results in V7HY7 being assimilated at 06z but rejected at 04z and the acceptance of the LNDSYN observation which was rejected in the cluster 1 experiments. These changes are due to differences in the buddy-checking criteria in which observations are accepted or rejected based on a consistency check with the observation's neighbours. Different results are observed throughout the six experiments, illustrating that bogus data can have unintended impact in the surrounding conventional observations and therefore on the analysis.

Figure 22 shows the results of the quality control for the u-component of the wind. It shows similar effects of the bogus data on the surrounding observations as discussed above. In particular the OPS will not allow both observations associated with clusters 4 and 5 through the quality control. The only case in which information from both observations are allowed through to the assimilation is in the control forecast in which all bogus observations of cluster 5 are assimilated along with the genuine observation associated with bogus cluster 4.

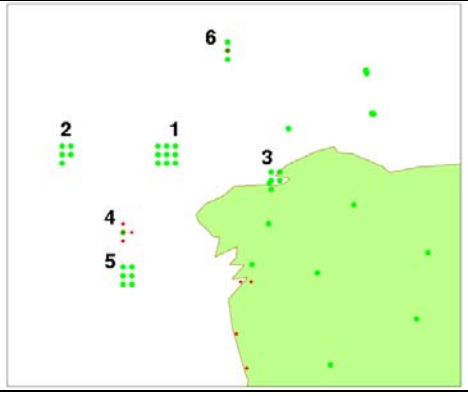

a) Cntrl (987, 989, 985)

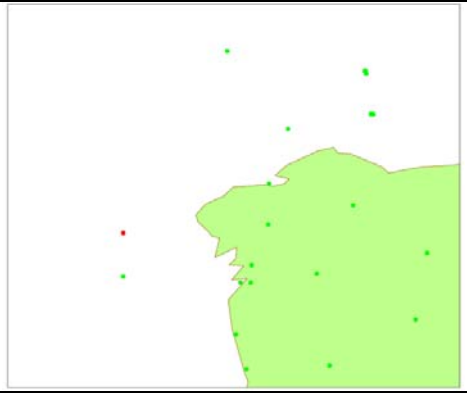

b) NO BOGUS (982, 979, 974)

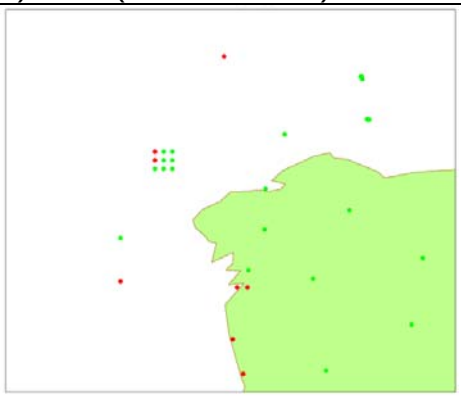

c) BOGUS 1 ONLY (983, 982, 979)

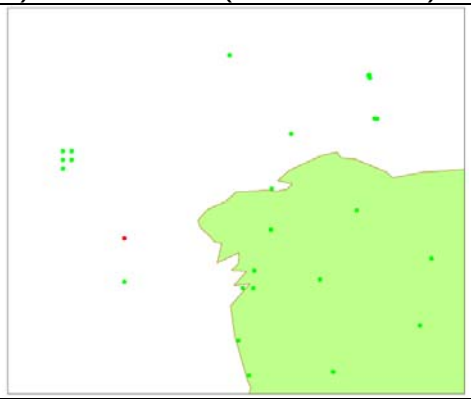

d) BOGUS 2 ONLY (986, 986, 983)

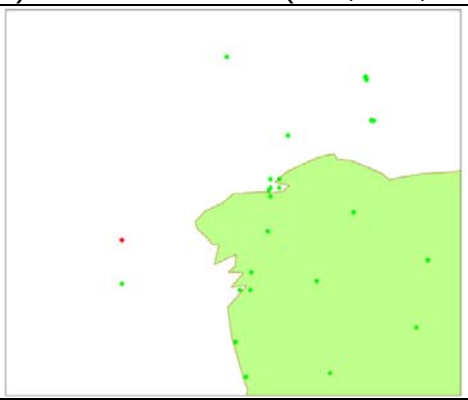

e) BOGUS 3 ONLY (982,980,977)

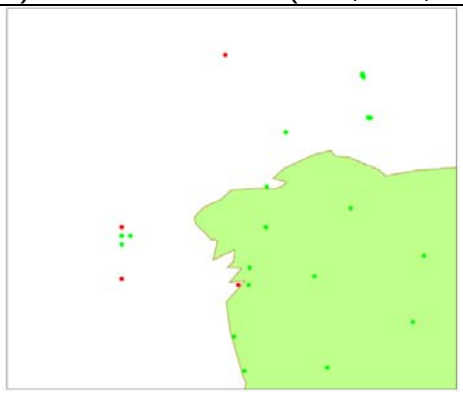

f) BOGUS 4 ONLY (975, 974, 973)

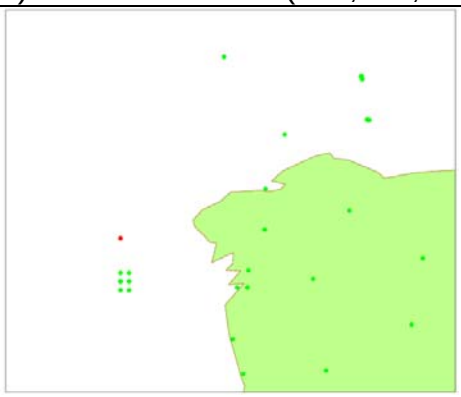

g) BOGUS 5 ONLY (989, 986, 982)

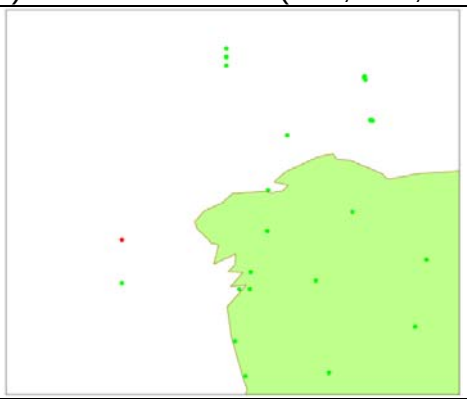

h) BOGUS 6 ONLY (985, 984, 980)

Figure 21 Quality Control from the OPS on pressure observations (green: accepted, red: rejected). The MSLP of the Gordon storm at T+0, T+6 and T+12 is shown in brackets.

Figure 22 As Figure 19 but for wind u-component.

Figure 23 shows the T+0 analysis fields resulting from the assimilation of each of the bogus clusters. The differences in the analysed lows resemble a spread of an ensemble which are perturbed about the depression represented in the 'no bogus'

run. Two outliers stand out in figure 23f, in which a low of 975hPa is located on the western boundary of the figure (and corresponding to the assimilation of cluster 4), and in figure 23g in which the low has been reduced to a shallow surface trough of ~989hPa (corresponding to the assimilation pf cluster 5).

The assimilation of bogus cluster 1 is an interesting case to consider because it consists only of pressure observations with no wind observations specified in the bogus data (this is because it represented the centre of the low). The result of assimilating the bogus data is a shift in the centre of the low southeastwards towards the Spanish coast and is consistent with the locations of the bogus data shown in figure 21a. The central MSLP of the low in the 'no bogus' run is 1hPa lower than the low in the 'cluster 1 only' run and results in a depression of 983hPa. This seems surprising, given that nine observations have been introduced into the assimilation of this run which are 6hPa below the background (see figure 5). However, the MSLP at the *location* of the bogus cluster 1 in the 'no bogus' run is 987hPa, whilst the MSLP at the *same location* in the 'cluster 1 only' run is 984hPa. This shows that there has been a decrease in MSLP corresponding to the bogus observations in the location of the bogus cluster as intended. The results are not necessarily as one might anticipate however, because of the necessity for the impact of the observations to spread both horizontally and vertically from their location and for VAR to achieve the best balanced state between the bogus observations and the surrounding global observations. As discussed earlier, there is the added complication that the introduction of the bogus observations affects the quality control decisions on the surrounding observations, such that different observations are rejected and accepted in the surrounding area and the assimilation 'sees' different observations. The result, therefore, is not necessarily a precise reflection of the anticipated effect on the analysis.

Figure 24 shows the central MSLP of the hurricane Gordon storm throughout the 12 hour forecast in each of the runs from these analyses. The NMC analysis is taken as 'truth'. The figure shows a wide spread in both the resulting analysis central surface pressure (spread of 14hPa) and the following T+6 (spread of 15hPa) and T+12 (spread of 13hPa) hour forecasts. The control run, with all bogus clusters assimilated, is the top curve of the figure, and generally represents the shallowest (and worst) of the solutions.

The run which is closest to the NMC truth is the cluster 3 only run, which were the only bogus data to be supporting a land-based pressure observation. This is 1hPa closer to the NMC analysis of the storm than the next most successful forecast: the 'no bogus' run.

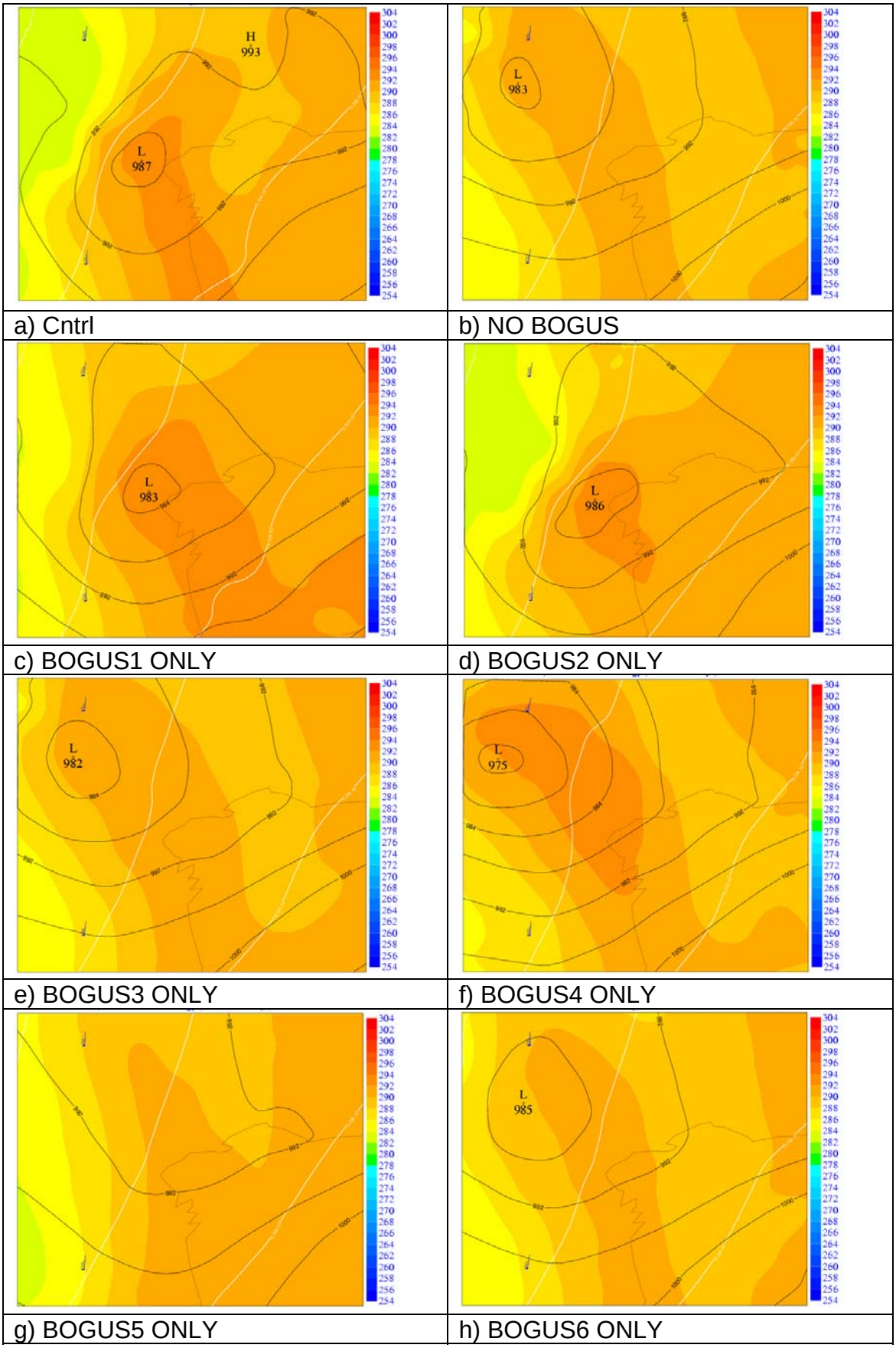

Figure 23 T+0 fields for the PS15 re-run experiments. Black contour: MSLP, White Contour: 250hPa gph, Colour: 850hPa theta-w.

The deepest low is a result of assimilating only bogus cluster 4, whereas the shallowest low at analysis time is that which assimilated only bogus cluster 5. Bogus clusters 4 and 5 are associated with the same observation two hours and ~40 miles apart so it is interesting that supporting one or other of them produces the two extremes of the solution at 14hPa apart. In part, this is understandable given that the two observations were taken before and after the storm moved through, and are 982hPa for the cluster 4 observations and 991hPa for the cluster 5 observations. The winds are also in the opposite direction (see figure 3). Clearly though, the assimilation system has struggled to represent the observations in the analysis.

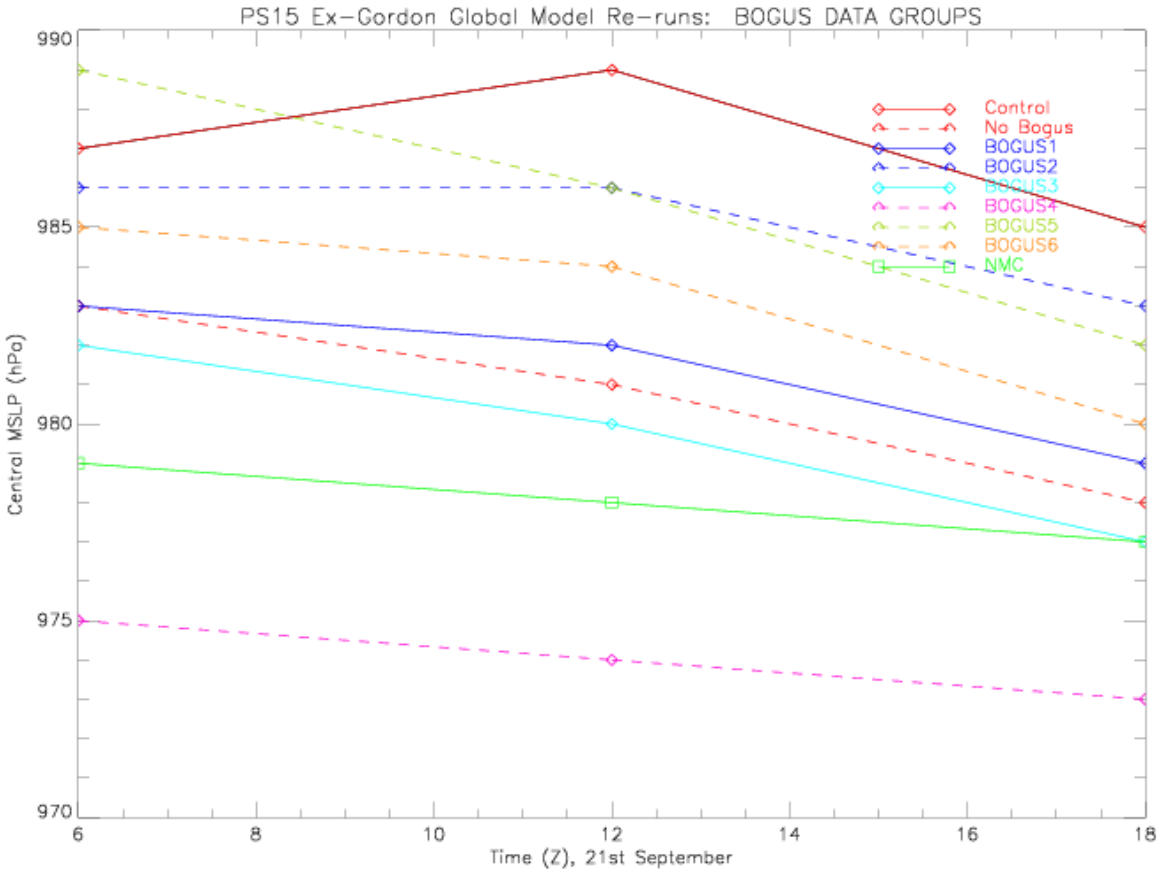

Figure 24 Central MSLP of the Hurricane Gordon remnant after assimilating each set of bogus observation clusters described in figure 19. 06z corresponds to the time of assimilation of the data, with 12z and 18z representing T+6 and T+12 respectively. The result is a large spread of forecast systems with a maximum difference of ~14hPa at analysis time and 13hPa at T+12.

The response of the analysis, and therefore of the subsequent forecast, to the assimilation of the different clusters is surprising, especially considering that four of the six clusters (3, 4, 5, and 6) merely support existing conventional observations.

A simplistic consideration of the assimilation process can explain some of the impacts of the bogus clusters but cannot explain all. For example, it seems reasonable that the six bogus observations of 982hPa in cluster 4 may result in an overall decrease in pressure at the analysis time, moving the curve to below the 'no bogus' curve. It also seems reasonable that the assimilation of cluster 5 with observations of 991hPa would move the curve up relative to the cluster 4 line. It is less obvious, why this would result in a much shallower low relative to the 'no bogus' line given that 4D-Var fits observations through the time window, and that the assimilation of either cluster 4 or 5 should be consistent.

There are three possible reasons which are offered as an explanation for the high sensitivity of the assimilation system:

- The resolution of the assimilation grid is ~1/3 that of the Global Model grid. This means that the entire area within the data coverage plots in figures 21 and 22 are within the area of one assimilation grid box. Although 4D-Var is treating the observations at their correct observation time, the overall result are increments that are, to a first approximation, a weighted mean of the results of all the observations within the assimilation grid box.

- 4D-Var assumes observation errors are uncorrelated. By creating a high-density region of identical observations this is effectively creating a region of observations which have correlated errors, and so invalidates one of the fundamental assumptions of the current assimilation scheme.

- Representivity of observations. The Gordon storm was of extra-tropical origin, and as such was a relatively small and fast moving system. It is possible for true observations, although accurate, to be non-representative of the larger scales on which the assimilation scheme (and indeed the model) operate. The result can be an analysis which perhaps is worse than if the observation was not assimilated at all.

Given that many of the bogus clusters of this case were supporting existing observations, this does not therefore suggest a problem with the generation and assimilation of bogus data per se but rather highlights the sensitivity of the assimilation to large numbers of closely packed identical observations. Depending on the contribution of each of the proposed reasons for the sensitivity in any one particular case, this would suggest unpredictable effects may result through the general use of bogus data.

9 Conclusions and Recommendations

During the extra-tropical transition of Hurricane Gordon, whilst the system was situated to the NW of Spain, heavy manual bogussing was used by Operations Centre in an attempt to improve the analysis. The manual bogussing data was based on an identified mismatch between the model and available satellite imagery and METAR reports.

It has been shown that this bogus data had a detrimental effect on both the analysis and the forecast in the operational system at the time (PS11). It has been shown that a forecast of considerably better skill would have been obtained if no manual bogussing had been carried out.

The effect of this bogus data on a more modern suite configuration (PS15) has also been shown to be detrimental. In this case however, the effect was more significant, with the developing low filling in response to the data during the subsequent six hour forecast. The result was a shallow surface trough instead of a well defined deep low. Indications are that this larger impact in PS15 relative to PS11 are due to different modelling of winds over land.

Further investigation into the PS15 case has shown that the analysis and forecasts are highly sensitive to the assimilation of each of the individual bogus observation clusters. A maximum spread of 15hPa central surface pressure of the Gordon Storm is observed at T+0 depending on which cluster is assimilated, which results in a spread of 10hPa at T+12.

This sensitivity is proposed not to be due to the use of bogus data per se but reflects the sensitivity of the analysis system to regions of high density identical observations.

With PS15 being shown to be more sensitive to the combined bogus observations than PS11, this indicates that the improved physics of the Unified Model is more sensitive to analysis differences introduced through this type of bogussing technique.

The unpredictable effects of bogussing on the analysis and forecasts is clear from this study. The single cluster assimilation experiments of PS15 show that it is possible to improve the analysis over a situation in which no bogus data is used. However, there is also five other cases in which the bogus data had a negative impact on the forecast. There is no reason apparent as to why the support of one observation would have a benefit over the support of an equally valid observation.

It is also possible that due to their relatively small scale and perhaps poorly modelled structures, that the bogussing of systems of extra-tropical origins such as in this case are an entirely separate case to the midlatitude systems. Without further work, however, it is not clear where the boundary between system types may be. It is therefore recommended that the continued conventional use of bogussing should be reviewed. In the short-term, this investigation suggests that the manual bogussing of systems of extra-tropical origin should be discouraged.

Operations Centre also carries out routine bogussing of data in which existing observations which are perceived as having a bias are supported with a ‘corrected’ bogus observation: the correction being based on a manual analysis of observation-background timeseries which are available as a diagnostic tool from the Data Assimilation group. This enables biases to be identified which have not been corrected by the automatic observation bias corrections and monthly station list updates. Providing large clusters of the bogus observation are not created, it would be understandable if there were some positive impact of this bogussing technique as it is based on timeseries statistics of the observations and may reduce cases in which poor observations are supported by a poor background.

10 Acknowledgements

The author wishes to thank Mike Thurlow for invaluable help and guidance in setting up the relevant suite configurations. Thanks to Tim Hewson who highlighted the case and for his contructive comments, and to Frank Saunders with help in Operations Centre and the testing of creating bogus data. Gratitude also to Andrew Lorenc, Rick Rawlins and Richard Renshaw for their discussions.